ChemCatChem

The European Society Journal for Catalysis

Chemistry Europe

European Chemical Societies Publishing

Supported by GECATS GERMAN CATALYSIS SOCIETY

Accepted Article

Title: In vivo reduction of medium- to long-chain fatty acids by carboxylic acid reductase (CAR) enzymes: limitations and solutions

Authors: Melissa Horvat and Margit Winkler

To be cited as: *ChemCatChem* 10.1002/cctc.202000895

Link to VoR: https://doi.org/10.1002/cctc.202000895

WILEY-VCH

10.1002/cctc.202000895

WILEY-VCH

FULL PAPER

In vivo reduction of medium- to long-chain fatty acids by carboxylic acid reductase (CAR) enzymes: limitations and solutions

Melissa Horvat[a] and Margit Winkler[a,b]*

[a] M. Horvat, Priv.-Doz. Dr. M. Winkler
acib - Austrian Center of Industrial Biotechnology
Krenngasse 37, 8010 Graz, Austria
E-mail: margit.winkler@tugraz.at
[b] Priv.-Doz. Dr. M. Winkler
Institute of Molecular Biotechnology
Graz University of Technology
Petersgasse 14, 8010 Graz, Austria

Supporting information for this article is given via a link at the end of the document.

Abstract: Fatty aldehyde production by chemical synthesis causes an immense burden to the environment. Within in this study, we explored a sustainable, aldehyde-selective and mild alternative approach by utilizing carboxylic acid reductases (CARs). CARs from *Neurospora crassa* (*Nc*CAR), *Thermothelomyces thermophila* (*Tt*CAR), *Nocardia iowensis* (*Ni*CAR), *Mycobacterium marinum* (*MmC*AR) and *Trametes versicolor* (*Tv*CAR) were overexpressed in *E. coli* K-12 MG1655 RARE (DE3) and screened for medium- to long-chain fatty acid (C6-C18) reduction. *MmC*AR showed the broadest tolerance towards all carbon-chain lengths and was selected for further investigations of fatty aldehyde synthesis in whole cells. To yield relevant product concentrations, different limitations of CAR whole cell conversions were elucidated and compensated. We coupled an *in vitro* cofactor recycling system to a whole cell biocatalyst to support cofactor supply and achieved 12.36 g L^{-1} of octanal (STY 0.458 g L^{-1} h^{-1}) with less than 1.5 % of 1-octanol.

Introduction

In the early 20th century, aldehydes were identified as crucial constituents of flavors and fragrances.[1] In particular, medium- and long-chain aliphatic aldehydes have ever since transformed the world of smells. In addition, aldehydes are seen as highly valuable intermediates in pharmaceutical industry[2] as well as precursors for products such as biofuels, biopolymers, etc.[3,4] The reactive nature of aldehydes is a challenge for their production: under oxidative conditions from alcohols, toxic catalysts are being employed,[5] and reductive routes from carboxylic acids suffer from poor atom economy and are prone to overreduction. Additional activation of the carboxylic acid group and protection of other reactive groups to minimize off-target reductions are in most cases required.[6] All these factors are cost contributors and cause an immense burden onto the environment.

In the biocatalysis community, a specific two-electron reduction of carboxylic acids to aldehydes by carboxylic acid reductases (CAR, EC 1.2.1.30) was discovered.[7,8] Bioreductions facilitated by CAR enzymes constitute a sustainable and environmentally-friendly alternative to chemical approaches.[9] Due to their broad substrate scope, including aromatic, aliphatic and heterocyclic carboxylic acids, CARs are gaining interest.[10–12] Structural analysis recently confirmed the catalytic steps in these enzymes that are composed of 3-domains.[13] First, the enzyme converts the substrate to an AMP-anhydride in the presence of ATP and Mg^{2+} in the adenylation domain (A- domain). Pyrophosphate is released. The AMP-anhydride is being targeted by the 4´phosphopantetheine moiety of the linker (peptidyl carrier protein (PCP) -domain) and the substrate is shuttled to the reductase domain (R-domain) as an enzyme bound thioester, while AMP is being released. In the presence of NADPH, the thioester is reduced to the respective aldehyde and released together with $NADP^+$.[14] For activation of the CAR enzyme, its apo-form needs to be phosphopantetheinylated by a phosphopantetheinyl transferase (PPTase) under coenzyme A (CoA) consumption to form active holo-CAR.

The necessity of PPTases to activate PCPs has been studied extensively. In nature, 4´-phosphopantethenylation is required for pathways forming toxins or primary and secondary metabolites.[15] Co-expression of PPTase with CAR enzyme was previously shown to enhance CAR activity and is seen as the gold standard.[14] Literature predominantly reports on the co-expression of *Sfp*PPTase with CAR enzymes. It is the best characterized PPTase with a wide substrate spectrum, which should interact with PCP-domains of diverse CARs,[16] but the activation of apo- to holo-CAR has not yet been addressed systematically.

Due to the dependency of the enzyme on cofactors, an *in vivo* approach as seen in the production of vanillin[17] seemed most feasible and cost-efficient in view of synthetic applications. To explore the suitability of CAR enzymes for the production of aliphatic aldehydes, the ideal process criteria would be the following: at least gram per liter production, a broad substrate acceptance by the enzyme, high biocatalyst yield/low biocatalyst requirement (< 0.005 g L^{-1} cell wet weight (CWW)), no by-products, no toxicity of substrates/products to the host organism, sufficient supply of cofactors, high intracellular concentrations of active CAR and a continuous process.[9] Several constraints were observed with the *in vivo* CAR approach for vanillin production by Hansen *et al.*[18] First, the metabolic flux of the carbon-source to vanillin in *de novo* synthesis was difficult to control. Similar difficulties in controlling the carbon flux were seen in the *de novo* synthesis of fatty acids, which have been described extensively.[19–21] The first and major challenge is targeting specific carbon-chain lengths of fatty acids.[3] A mixture of fatty acids will result in a mixture of the respective aldehydes in a reaction sequence with CARs due to the enzyme´s broad substrate scope. In case of individual aldehydes as desired products, the use of living cells in biotransformation mode (feeding carboxylic acids) is typically more efficient compared to

the *de novo* approach, due to the limited carbon flux to the desired fatty acid as CAR substrate.[19] Herein we focused on this strategy.

The second challenge was that the host organisms showed high levels of aldehyde overreduction by alcohol dehydrogenases (ADHs) and/or aldo-keto reductases (AKR) (Figure 1).[18] Overreduction of aldehydes to alcohols (Figure 1) is the intracellular defense-mechanism of the expression host for coping with high concentrations of these toxic compounds.[22] Of the respective acid, aldehyde and alcohol, the fatty acid is the most tolerated compound.[23] However, relatively low concentrations of aliphatic acids and derivatives cause growth inhibition, cell membrane perforation and leakage, thus disrupting the electron transport chain, uncoupling oxidative phosphorylation and ultimately diminish ATP production.[24] 30 mM octanoic acid, e.g., caused 46% of increased leakage of ions in *E. coli* K-12 MG1655 cell membranes. Perforation of the cell membranes is the result of a missing defense strategy in *E.coli*.[25,26]

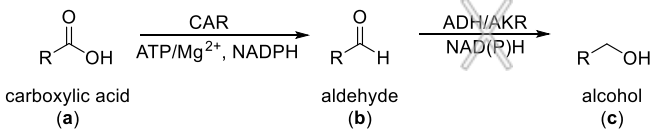

Figure 1. Reduction of carboxylic acids to aldehydes and overreduction to alcohol.

The majority of literature reports on alcohols as the desired products of CAR mediated acid reductions. For example, Akthar *et al.* were the first to describe the medium- to long-chain fatty acid reduction by *Mycobacterium marinum* CAR to a mixture of fatty alcohols and alkanes for *de novo* biofuel production in milligram-scale.[27] Ahsan *et al*. targeted fatty diols by utilizing an enzyme cascade incorporating endogenous aldehyde reductase activity of *E. coli*. By doing so, 4.6 g L^{-1} of 1,12-dodecanediol, a very important monomer for polyester production, were produced, demonstrating the feasibility of gram-scale production with a whole cell catalyst. However, 30 OD units (~30 mg mL^{-1} CWW) of *E. coli* were applied and production of 1,8-octanediol resulted in only 0.56 g L^{-1} product concentration. The explanation for decreased product titer might be increased toxicity of the shorter carbon-chain compound compared to 1,12-dodecanediol.[28] Further, a study targeting C10-C12 aldehydes could not limit overreduction to less than 80% in *E. coli* MG00 of *E. coli* K-12 MG1655 origin.[29]

Targeting aldehydes, Hansen *et al.* established an enzyme cascade to produce vanillin glucoside which is the naturally occurring compound in vanilla pods, via *de novo* biosynthesis.[18] Additionally, yeast strains used for vanillin glucoside production were engineered to minimize overreduction to vanillyl alcohol. ADH and AHR genes responsible for overreduction of vanillin were identified and deleted. In a similar study, the *E. coli* K-12 MG1655 (DE3) strain was modified for aromatic aldehyde accumulation by using the same approach.[30]

As an alternative to cellular systems, CAR mediated synthesis of aldehydes was recently shown. ATP is recycled *in vitro* with two polyphosphate kinases, and NADPH by exploiting a commercially available GDH. For eliminating the CAR inhibitor pyrophosphate from the reaction, a pyrophosphatase from *E. coli* was also implemented.[31] In similar approaches, cascade reactions were investigated to pull the aldehyde intermediate from the reaction towards follow-up products. Because of impurities in enzyme preparations alcohol by-products were observed.[32,33] Fatty amines were targeted by Citoler *et al.* in a one-pot tandem cascade performed by a CAR and a transaminase, while recycling NADPH and ATP. In order to achieve high fatty amine concentrations, an *in situ* product removal system (ISPR) was applied and an end product yield of 0.927 g L^{-1} dodecyl amine was achieved.[33] ISPR is used to trap the compounds in the organic layer and to improve product yields by reducing the exposure of the cells to the cytotoxic compounds.[34,35] Due to decrease in cell viability when organic solvents are used for ISPR, biocompatible solvents can be beneficial to achieve high product titers. Cell viability ensures intracellular cofactor regeneration, and biocompatible solvents could be highly advantageous in this respect.[36]

An optimized whole cell system for acid reduction to fatty aldehydes as end products is of high demand, but only few studies actually describe targeting fatty aldehydes. With the exception of Hansen *et al*.,[18] no study aimed for a comprehensive picture of advantages and limitations of CAR mediated whole cell applications aiming for aldehyde products. In this study, CAR enzymes from *Neurospora crassa* (*Nc*CAR),[34] *Thermothelomyces thermophila* (*Tt*CAR),[37] *Nocardia iowensis* (*Ni*CAR),[38] *Mycobacterium marinum* (*Mm*CAR)[27] and *Trametes versicolor* (*Tv*CAR)[39] were overexpressed in *E. coli* K-12 MG1655 RARE (DE3) and screened for medium- to long-chain fatty acid (C6-C18) reduction. *Mm*CAR showed the broadest tolerance towards all carbon-chain lengths and was selected for further investigations of fatty aldehyde synthesis in whole cells. To yield relevant product concentrations, a systematic evaluation of various parameters of both the cultivation phase and the biotransformation phase were carried out.

Results and Discussion

Substrate scope of CARs in single phase reactions *in vitro*

A toolbox of CARs is available today for enzymatic reduction of carboxylic acids to aldehydes. For production of fatty aldehydes, the most suitable CAR needed to be identified. Therefore, fungal and bacterial CARs of three phylogenetic groups[40] were screened for fatty acid reductase activities. The substrate specificity of CARs was described to be determined by the adenylation core domain of CARs.[41] Because sequence similarities between different subtypes and between fungal and bacterial origins are below 25%, substrate spectra vary.[40,42]

Substrate solubility limited the spectrophotometric assay to medium chain aliphatic acids. Moreover, NADPH depletion is only an indirect method. Chromatography based methods directly detect the desired aldehyde **b** and possible alcohol **c** as a result of over-reduction. An *in vitro* activity assay method was developed for quantitation of unreacted acid **a**, desired aldehyde **b** and undesired alcohol **c** using gas chromatography (GC). Due to the lack of commercially available product standards, substrates without product standards were measured via gas chromatography-mass spectrometry detection (GC-MS). All other fatty acids, aldehydes and alcohols were quantified with gas

chromatography-flame ionization detection (GC-FID) using calibration curves.

Figure 2 summarizes the substrate scope of CARs. First, almost all CARs converted all listed compounds in Figure 2 at least in trace amounts. This highlights the broad substrate tolerance of CARs. Substrate preferences agreed well with literature. Type III *Nc*CAR was outstanding for hexanoic acid **1a** (Figure 2). Type IV *Tv*CAR had shown a tendency towards aliphatic substrates in comparison to other type IV CARs such as *Ds*CAR and *Tv2*CAR.[37] Second, as indicated by color, short chain aliphatic acids (hexanoic acid **1a** and heptanoic acid **2a**) showed high conversions compared to low conversions of long-chain fatty acids (oleic acid **14a** and linoleic acid **15a**). Especially *Nc*CAR showed outstanding activity with **1a**. When it comes to medium-chain substrates (octanoic acid **3a**, nonanoic acid **4a**, 4-methylnonanoic acid **5a**, 8-methylnonanoic acid **6a**, decanoic acid **7a**, 9-decenoic acid **8a**, undecanoic acid **9a**, 10-undecenoic acid **10a**, and 5Z-dodecanoic acid **11a**), type I (*Mm*CAR and *Ni*CAR) and IV (*Tv*CAR) CARs outperform type III CARs (*Nc*CAR and *Tt*CAR). Comparing branched and unbranched substrates **4-6a**, the presence of a terminal methyl-group (**6a**) increased conversion, whereas a branch in the middle of the carbon chain (**5a**) reduced product formation with all CARs. The best *in vitro* conversions were observed for **6a**. Long-chain aliphatic substrates (myristoleic acid **12a,** palmitoleic acid **13a** and oleic acid **14a**) were mostly accepted by bacterial and type IV fungal CARs. As a general trend, CARs performed better with unsaturated substrates compared to saturated compounds. This was also observed in Citoler *et al.* in cascade reactions to fatty amines.[33] Further, short-chain aliphatic substrates were more accepted by type III CARs, whereas long-chain aliphatic substrates were best accepted by type I bacterial CARs .

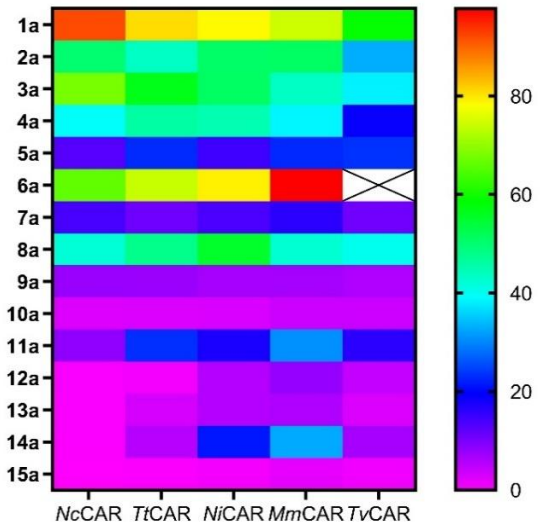

Figure 2. Substrate scope of CARs towards saturated, unsaturated and branched fatty acids: hexanoic acid **1a**, heptanoic acid **2a**, octanoic acid **3a**, nonanoic acid **4a**, 4-methylnonanoic acid **5a**, 8-methylnonanoic acid **6a**, decanoic acid **7a**, 9-decenoic acid **8a**, undecanoic acid **9a**, 10-undecenoic acid **10a**, 5Z-dodecenoic acid **11a**, myristoleic acid **12a**, palmitoleic acid **13a**, oleic acid **14a** and linoleic acid **15a**. Substrates **5a, 6a, 8a, 11a, 12a** and **14a** and **15a** were detected with GC-MS all others via GC-FID. (Retention times and chemical structures are summarized in Table S6 and S7). X not determined.

Single-phase bioreduction of *E. coli* whole cells expressing *Mm*CAR and *Ec*PPTase

Recently, biosynthesis of fatty acids and derivatives is gaining attention due to their potential of replacing petroleum-based process.[3,43] We aimed for an *Mm*CAR producing *E. coli* biocatalyst in *in vivo* to take advantage of cellular metabolism for ATP and NADPH supply.

E. coli K-12 MG1655 RARE (DE3) had been engineered towards reduced overreduction of aromatic aldehydes, such as benzaldehyde and vanillin, to the respective alcohol by knocking-out six alcohol dehydrogenase and aldo-keto reductase genes and one activator gene by Kunjapur *et al.* A 55-fold improvement in vanillin titers compared to the wild type strain was achieved.[30] This strain seemed promising for aliphatic aldehyde production as it also showed less overreduction of octanal.[44]

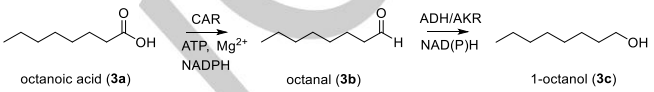

Figure 3. Reduction of the model substrate octanoic acid (**3a**) to octanal (**3b**) and overreduction to 1-octanol (**3c**).

First bioreductions were conducted with this strain, harboring a single plasmid for co-expression of *Mm*CAR and *Ec*PPTase. Certain OD units of the *E. coli* strain co-expressing PPTase and *Mm*CAR were harvested and resuspended in reaction buffer. Substrate and additives were added. After incubation of the bioconversions at 28°C, the aqueous solution was extracted twice with ethyl acetate and internal standard and measured via GC-FID. Figure 4 shows full conversion of 6 mM **3a** after 4.5 h at 28°C with 50 OD units (corresponding to approximately 50 mg of cell wet weight (CWW)). Independent of cell density, the product was almost exclusively **3c**, indicating that the engineered *E. coli* strain still harbors alcohol dehydrogenases and aldo-keto reductases with the ability for **3b** reduction (Figure *3*). Bioreductions with 100 OD units showed poor mass balance already after 4.5 h, which could be due to its utilization as a C-source. Up to 5.82 mM of 1- octanol (97.0%) was detected under these conditions via GC-FID. This correlates to a productivity of 0.745 g L^{-1} or a space time yield of 0.165 g L^{-1} h^{-1}.

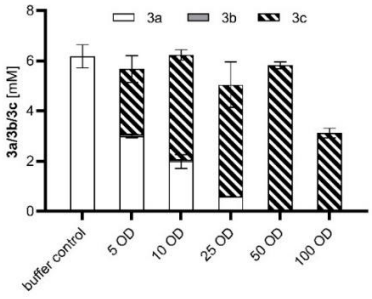

Figure 4. Single-phase bioreduction of *E. coli* K-12 MG1655 RARE (DE3) expressing *Mm*CAR and *Ec*PPTase with different cell densities converting 6 mM **3a**. 50 OD units correspond to approximately 50 mg cell wet weight (CWW). Bioconversions were incubated at 28°C for 4.5 h on a tissue culture rotator. White: **3a.** Grey: **3b.** Black striped: **3c** (see Figure 3 for reaction scheme)**.** Error bars are shown for biological triplicates.

Time dependent reactions with 50 OD units of biocatalyst

This first experiment revealed the challenge to obtain aldehyde instead of alcohol despite the CARs product selectivity. We previously showed that *in situ* product removal (ISPR) with *n*-hexane suppressed cinnamyl alcohol formation to the benefit of cinnamaldehyde titers.[34] Using a second organic layer puts additional constraints on the biotransformation itself as well as on the industrial applicability, such as process robustness, safety aspects (e.g. flammability of solvents) and the market of the product.[35] Furthermore, organic solvents such as *n*-hexane and *n*-heptane, are cytotoxic.[33,34,45] This includes growth inhibition, due to interaction of the solvent with cell membranes. Effects on cell integrity and cell vitality must, therefore, be expected in an ISPR approach with living (*i.e.* ATP regenerating) cells. However, trapping the aldehyde in an organic layer to reduce its harming effects increased cell vitality and integrity compared to a single-phase system and therefore increased conversion levels and aldehyde titers (Figure 5). A number of non-water miscible solvents were tested for ISPR. A positive trend towards **3b** production was observed. A second organic layer resulted in at least 50% of **3b** formation. After 3 h, full conversion was observed for short-chain alkanes as second layer (*n*-hexane and *n*- heptane), whereas only 80% of **3a** was converted using *n*- dodecane as trapping layer. The mass balance indicated that **3a**, **3b** and **3c** were fully extracted from the aqueous phase. Decreased formation of **3c** indicates that **3b** is efficiently exported from the cells and detoxification by over-reduction is the secondary mechanism after **3b** expulsion.

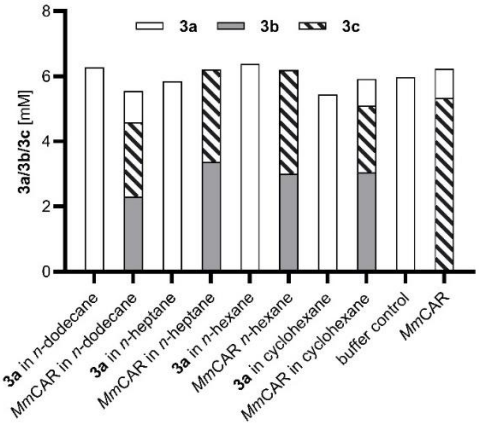

Figure 5. Biphasic bioreduction converting 6 mM of **3a** for aldehyde trapping and comparison to single phase reaction. 50 OD units of *E. coli* K-12 MG1655 RARE expressing *Ec*PPTase and *Mm*CAR were incubated at 28°C for 3 h on a tissue culture rotator. White: **3a**. Grey: **3b**. Black striped: **3c** (see Figure 3 for reaction scheme). Quantification by GC-FID.

Building on the positive effect of ISPR on aldehyde formation, we next increased substrate concentrations. After 18 h, 30.8 mM **3b** and **3c** were produced from 50 mM of **3a** (Figure S2). This correlates to a productivity of 3.0 g L^{-1} or 0.168 g L^{-1} h^{-1}. Evident from Figure S2, *in vivo* CAR reactions discontinued after few hours. When aldehyde formation stops, surplus NADPH leads to depletion of the desired product and alcohol formation. Possible reasons for preliminary stop of acid reduction may be poor stability of the CAR or limited ATP and NADPH supply due to the effects of solvent, products and/or substrate on cell viability. To improve the reaction system, we investigated these hypotheses.

Overreduction, a mechanism to minimize cytotoxicity of certain compounds by the cell, constantly interfered with aldehyde titers. For this reason, not many studies focused on fatty aldehydes as the final product.[46] On the contrary, they exploited this effect to optimize fatty alcohol [28,47] or alkane[27,48] titers. To overcome overreduction of fatty aldehydes, we screened 30 single deletion *E. coli* BW25113 strains from the Keio Collection[49] to find a strain, which might have a decreased defense mechanism for fatty aldehydes (data not shown). Especially genes coding for alcohol dehydrogenases and aldo-keto reductases were chosen as targets. By incubation of the strains with medium- to long-chain fatty aldehydes and determining alcohol concentrations, strains with low alcohol concentrations should give indications of genes responsible for overreduction of fatty aldehydes. Next to aldehyde overreduction, also aldehyde oxidation to its respective fatty acid was observed, which was most likely due to aldehyde dehydrogenases.[50] In the best-case scenario, only one or two genes would be identified as responsible for overreduction of fatty aldehydes and would need to be engineered in the *E. coli* genome for aliphatic aldehyde production. In Table S1 the four gene deletion strains with the lowest alcohol concentrations for five substrates (**3a**, **7a**, **9a**, **10a** and **13a**) were compared to *E. coli* K-12 MG1655 RARE (DE3). None of the non-essential genes of the Keio collection seems to exhibit the exclusive reduction capacity for any of the tested substrates. A single gene deletion is certainly not enough for any of the investigated substrates to fully suppress alcohol formation.

To our delight, *E. coli* K-12 MG1655 RARE (DE3) was the best strain in this comparison. It was interesting to observe that gene deletions of *yahK, yjgB, yqhC* and *yqhD* in the *E. coli* K-12 MG1655 RARE strain was found beneficial for minimizing overreduction of fatty aldehydes, specifically **3a**, in this study. Deletions of *yeaE, dkgB* and *dkgA* might be specific to aromatic substrates, because these genes did not show a positive effect for aliphatic aldehyde reduction.

Reduced biocatalyst amount resulted in less than 1% overreduction

Next, we aimed to determine the optimal biocatalyst concentration. High biocatalyst amounts introduce more CAR, but less biomass in the biotransformation should decrease endogenous co-factor pools and enzymes with aldehyde reductase activity. Indeed, by reducing biomass to 1-5 OD units of *E. coli* K-12 MG1655 RARE (DE3) expressing *Ec*PPTase and *Mm*CAR, only ~ 1% of **3c** was formed within 5 h (Table 1, Figure S3), at reduced **3b** formation. Bioconversions with 50 OD units of *E. coli* cells expressing CAR and PPTase showed nearly 60% of **3c**. For industrial applications, biomass is a major cost-factor. Hence, a reduction of biocatalyst to keep alcohol formation low would be beneficial for multiple reasons.

Table 1. Product formation of biphasic bioreduction of 10 mM **3a** with increasing amount of *E. coli* MG1655 RARE cells, co-expressing *Ec*PPTase and *Mm*CAR.

	1 OD	2 OD	5 OD	10 OD	20 OD	50 OD
3b+3c [mM][a]	0.10	0.23	0.48	0.93	1.75	3.30
3c in product [%][a]	1	1	1	8	26	59

[a]All standard deviations were <0.1%. Technical triplicates were measured via GC-FID.

Table 2. Comparison of *Mm*CAR expression at different temperatures.

Expression parameters of *Mm*PPTase and *Mm*CAR	CWW per 450 ml cultivation [g]	*In vivo* product formation of **3b+3c** [mM][a]	Partially purified enzyme yield [mg]	specific activity for **3a** [U/mg]
auto induction at 20°C	5.91	6.02 ± 0.20	42.1	0.32± 0.02
auto induction at 25°C	6.15	5.50 ± 0.23	64.9	0.18± 0.01
auto induction at 28°C	6.53	3.21 ± 0.17	55.8	0.10± 0.03

[a]Conditions for biotransformation: 24 h post induction, 50 OD units, biphasic setup, 28°C, tissue culture rotator, 3 h, 6 mM **3a**, quantification via GC-FID, standard deviations are shown for three biotransformation reactions.

CAR-expression and activation

A further increase in biocatalyst efficiency was expected by increasing the levels of functional *Mm*CAR in the cells. The co-expression of a PPTase is vital to obtain functional CAR (Figure S4).[14] Without co-expression of a PPTase only 4.6% of activity was observed compared to 100% activity with co-expressed PPTase (Figure 7). In our hands, higher soluble expression levels of *Mm*CAR did not correlate to higher activity levels (Table 2). Partially purified CARs that were produced at either 20°C, 25°C or 28°C showed that the highest yield of soluble *Mm*CAR was obtained at 25°C (64.9 mg). However, highest specific activity was clearly obtained with *Mm*CAR produced at 20°C.

Incorrectly folded proteins should be found as inclusion bodies,[51] however, folding was not a limitation for *Mm*CAR, since soluble protein content increased. Consequently, we hypothesized that insufficient posttranslational modification would lead to inhomogeneous CAR, in other words, a mixture of soluble non-activated apo-CAR and activated holo-CAR. Hence, the soluble *Mm*CAR expressed at 25°C would have a higher content of apo-CAR compared to holo-CAR, whereas CARs expressed at 20°C have a higher portion of holo-CARs. To examine this assumption, *in vitro* studies of partially purified *Mm*CAR were conducted. If the *Mm*CAR preparation undergoes 4´-phosphopantetheinylation *in vitro*, the specific activity of the preparation should increase and deliver a first evidence of the presence of apo-CAR despite co-expression of PPTase.

***In vitro* activation of *Mm*CAR with *Gk*PPTase**

Partially purified *Mm*CAR, was additionally activated *in vitro* with a novel, thermostable PPTase from *Geobacillus kaustophilus* and CoA for 1 h before *Mm*CAR activity was determined (Figure 7). Partially purified *Mm*CAR had been co-expressed with *Ec*PPTase prior purification and *in vitro* activation with *Gk*PPTase. Cloning details of *Gk*PPTase can be found in supplementary information, section Materials and Methods. *Gk*PPTase was purified by heat-precipitation of background proteins before use.

The *in vitro* post-translational modification of purified *Mm*CAR by *Gk*PPTase in the presence of CoA clearly increased activity (Figure 7). *Mm*CAR expressed at 20°C showed 70% conversion, which was increased by 10% by *in vitro* activation. Fifty percent conversion was achieved by enzyme preparations expressed at 25°C, which could be increased to full conversion of 6 mM **16a**. Consequently, the holo-CAR fraction must have been doubled. The increased activity confirms that CAR expression at both temperatures resulted in a mixed population of apo-CAR and holo-CAR. At low expression temperature (20°C), 4´-phosphopantetheinlation by endogenous and overexpressed *Ec*PPTase is efficient, but not exhaustive. By increasing the expression temperature to 25°C more soluble CAR molecules were produced due to higher efficiency of the expression machinery of *E. coli* at this temperature. However, posttranslational modification of *Mm*CAR seemed to become insufficient. Correctly folded CAR proteins are necessary for Sfp-like PPTases such as *Ec*PPTase. PPTases recognize PCP protein structure and not only the primary amino acid sequence. This was the conclusion by studying the interactions of PCP mimic polypeptides of the conserved sequence (19AA) or whole PCP proteins.[15] Several studies of carrier proteins and their 4´-phosphopantetheinylation described that apo- and holo-carrier polypeptides were both found in cell lysates. The ratio of apo- to holo- carrier protein was directly linked to the presence or activity of PPTases. Additionally, it was speculated that the amount of apo- to holo- carrier proteins regulates metabolic processes.[52] This supports the assumption that different ratios of correctly folded apo- and holo-CARs could be present in the soluble fraction dependent on the amount and the efficiency of the PPTase.

For activating CAR molecules not only the presence of a PPTase plays an important role, but also intracellular CoA is required.[15] Because equimolar concentrations of apo-CAR and CoA molecules are necessary for full modification by PPTases,[14] high soluble CAR concentrations will lead to CoA depletion. It was described that decreasing CoA levels activated the acyl carrier protein hydrolase (AcpH, also called ACP phosphodiesterase) in *E. coli* and AcpH removed the 4´- phosphopantetheine arm from its carrier protein.[53] This regulation mechanism may be one reason for high apo-CAR content under conditions of strong expression. Two possible investigations for improved modification of apo-CARs would be attractive: increased CoA levels for higher holo-CAR concentration and the identification of a PPTase with improved apo-CAR activation potential.

The optimal PPTase for improved *Mm*CAR activation

Up to date, the PPTase *Sfp* from *Bacillus subtilis*, the name giving PPTase of the subclass comprising PPTases for the activation of CARs, has been studied and applied most extensively. *Sfp* was shown to be able to modify all types of carrier proteins and has a K_m of 0.7 µM and a k_{cat} of 102 min^{-1} for the co-substrate CoA, which is the 4´-phosphopantetheinyl group donor (Figure S4).[16] It showed a clear pH optimum at pH 6.0 with activity loss of more than 70% at pH 5.0 or 7.0.

10.1002/cctc.202000895

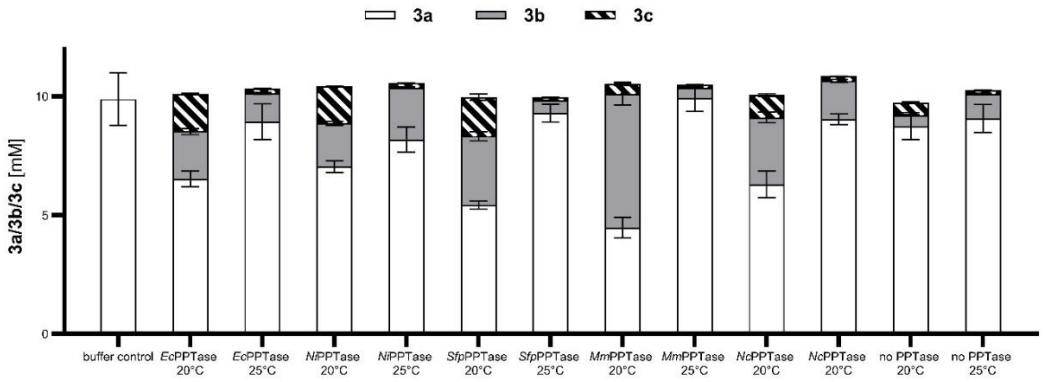

Figure 6. Biphasic bioreductions with 50 OD units of *E. coli* K-12 MG1655 RARE expressing *Mm*CAR and 5 different PPTases at 20°C or 25°C. Bioconversions were conducted with 10 mM **3a**, at 28°C for 3 h on a tissue culture rotator. White: **3a**. Grey: **3b**. Black striped: **3c** (see Figure 3 for reaction scheme)**.** Error bars are shown for biological triplicates.

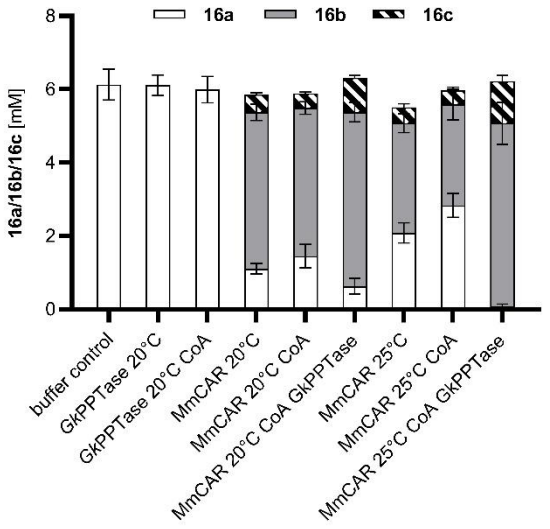

Figure 7. *In vitro* conversions of 6 mM **16a**. *Mm*CAR and *Ec*PPTase, were co-expressed at 20°C or 25°C. *Mm*CARs were purified and pretreated with heat-purified *Gk*PPTase and CoA. Activation time: 1 h. Reaction time: 3 h at 28°C. Triplicates were measured via HPLC-UV at 254 nm. White: **16a**. Grey: **16b**. Black striped: **16c**.

In *E. coli*, the homologous gene for transcribing the Sfp-type PPTase was identified as *entD*. This *Ec*PPTase was used as the co-expressed PPTase for activation of apo-CARs in this and other studies.[18,34,37,54,55] To co-express a PPTase that binds and activates the PCP-domain from *Mm*CAR perhaps more efficiently than *Ec*PPTase, the endogenous PPTases from known CAR origins (*Nocardia iowensis*, *Neurospora crassa*, *Mycobacterium marinum*) as well as *Sfp*PPTase from *Bacillus subtilis,* which was widely used in CAR research,[12,27,56,57] were cloned and co-expressed with *Mm*CAR. Biphasic whole cell bioconversions of **3a** were carried out to study the effect. Specifically, co-expression at 20°C and 25°C was performed in *E. coli* K-12 MG1655 RARE to compare activities of cells with high amounts of soluble CAR (produced at 25°C) to rather low amounts (produced at 20°C).

In accordance with earlier results, high amounts of soluble *Mm*CAR were produced at 25°C and lower amounts of soluble protein when expressed at 20°C (Figure S5). When activities were compared, it was apparent that more soluble CAR again (Figure 6) corresponded to significantly less activity, either due to incorrect folding or lack of essential decoration. Comparing the different PPTases, activity levels varied. The best conversions were observed by *Mm*CAR modified by either *Sfp*PPTase (45.6%) or *Mm*PPTase (57.6% conversion), both clearly outperforming *Ec*PPTase (35.5%). A 1.6-fold improvement was achieved. These results indicate that in case of *Mm*CAR, its native PPTase from *Mycobacterium marinum* seems to be a better choice for activating apo-*Mm*CAR to holo-*Mm*CAR.

Interestingly, high expression levels of (soluble) PPTases did not increase activation of apo-*Mm*CAR. The expression level of *Mm*PPTase at 20°C, for example, showed a small PPTase protein band compared to *Nc*PPTase expressed at 20°C (Figure S6). However, higher activity levels were detected with *Mm*PPTase, suggesting that interaction of the PPTase with the CAR was more important than its mere amount.

Despite this improvement, insufficient 4´- phosphopantetheinylation at higher expression temperatures was – by far – not fully compensated, suggesting that the intracellular CoA pool might be limiting.

Precursor supplementation to increase CoA supply

CoA is, at least, needed equimolar to apo-CARs.[14] The biosynthesis pathway of CoA in *E. coli* (Figure S7)[58] is highly energy-consuming: to form one molecule of CoA, one NADPH and four ATPs are required. According to literature, one of the major rate-controlling steps is the conversion of pantothenate to 4´- phosphopantothenate by the pantothenate kinase PanK (also known as CoaA).[59] CoA concentrations regulate PanK activity by competing for the ATP binding site.[60] Therefore, the energy state of the cells plays an important role. High intracellular ATP levels will increase concentrations of CoA levels available for 4´- phosphopantetheinylation and override the competitive behavior of CoA.[61] This interaction between ATP and CoA levels lead to the hypothesis that an increase in CoA level during expression would most likely be beneficial for the formation of holo-CAR.

Table 3 Comparison of *Mm*CAR expression with supplementation of D-pantothenate at different temperatures.

Expression parameters of *Mm*PPTase and *Mm*CAR	5 mM of supplementation	CWW per 450 ml cultivation [g]	*In vivo* product formation of **3b**+**3c** [mM]*	IMAC purified enzyme yield [mg]	specific activity for **3a** [U mg $^{-1}$]
autoinduction at 20°C	L-valine	5.73	3.91± 0.74	52.9	0.20± 0.02
autoinduction at 20°C	β-alanine	5.82	1.95± 0.94	43.6	0.28± 0.03
autoinduction at 20°C	L-aspartate	5.79	4.65± 0.15	46.7	0.29± 0.05
autoinduction at 20°C	D-pantothenate	5.89	16.7± 1.17	48.9	0.85± 0.08
autoinduction at 25°C	D-pantothenate	6.39	21.4± 0.40	67.0	0.76± 0.05
auto induction at 28°C	D-pantothenate	6.65	14.6± 0.13	49.7	0.70± 0.06
auto induction at 20°C	No precursor	5.91	6.02 ± 0.20	44.1	0.27± 0.04

*Conditions for biotransformation: 24 h induction, 5 OD units, 28°C, tissue culture rotator, 3 h, 30 mM of **3a**, determined via GC-FID, standard deviations are shown for triplicates.

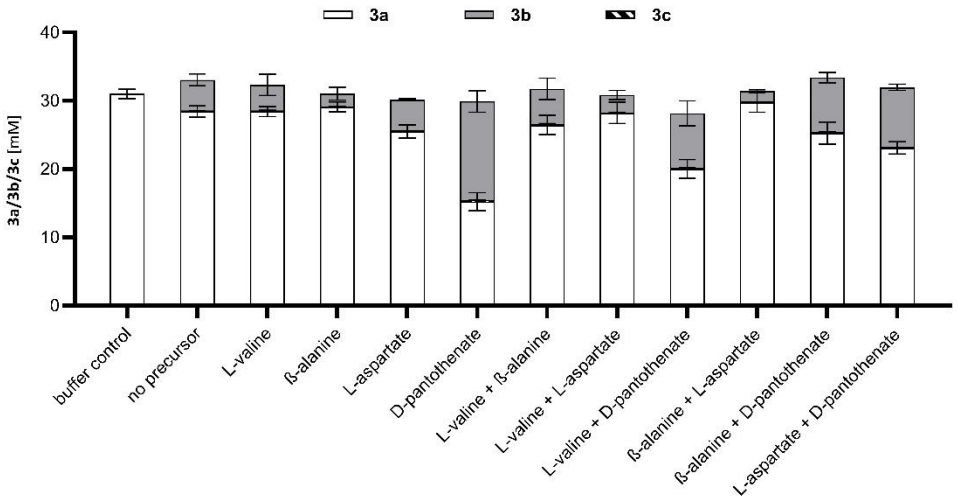

Figure 8. Effect of CoA precursor supplementation during induction on biphasic bioreductions. 5 OD units of *E. coli* K-12 MG1655 RARE expressing *Mm*CAR and *Mm*PPTase were incubated with 30 mM **3a** at 28°C for 16 h. White: **3a**. Grey: **3b**. Black striped: **3c** (see Figure 3 for reaction scheme). Error bars are shown for biological triplicates.

To increase CoA levels, inexpensive precursors of CoA were supplemented into growth and/or CAR expression media and the effect on carboxylate reduction capacity of the whole cell biocatalyst was examined. Because most bacteria, including *Escherichia coli* synthesize pantothenate, the key intermediate in CoA biosynthesis, from the amino acid L- aspartate and an intermediate in L-valine biosynthesis,[62] L- aspartic acid and L- valine were tested. L- Aspartate is decarboxylated to β- alanine in intact cells and further coupled to pantoate to form pantothenate.[63] Therefore, L- aspartate, L- valine, β- alanine and D- pantothenate were supplemented. Five mM of each and selected combinations were added either directly into the growth media or supplemented before expression was initiated. To study the effect, 5 OD units of *E. coli* cells were used for biphasic bioreductions to assess activity and indirectly the amount of holo-CAR. Supplementation of CoA precursors at the begin of *E. coli* cultivation only resulted in slight increase of CAR activity (Figure S8). However, supplementation of precursors and combinations thereof at the begin of the expression phase showed improved activities compared to *E. coli* K-12 MG1655 RARE (DE3) expressing *Mm*PPTase and *Mm*CAR without supplementation (Figure 8, no precursor). *E. coli* cells without addition of precursors showed conversions of 14%, similarly to cells supplemented with either L- valine, β- alanine and/or L- aspartate. Surprisingly, cells expressed with additional D- pantothenate showed conversions of 49% forming 14.6 mM of **3b** (and minor amounts of **3c**), suggesting that the increase in activity by 35% was due to higher holo-CAR content. All supplementations of D- pantothenate with either L- valine, β- alanine or L- aspartate showed increased activities of about 24% to 29%. Therefore, supplementation of solely D- pantothenate improved CAR activation the most.

It was reported that *E. coli* is not growth inhibited when precursors such as pantothenate were supplemented.[64] This observation was confirmed herein (Table 3). Equal amounts of CWW (~5.8 g) were harvested from 450 mL cultures, incubated at 20°C during the expression phase. Further, protein yields of CARs in *E. coli* with or without supplementation were compared (Table 3).

CAR expression at 20°C yielded ~45 mg of Ni-affinity chromatography purified CAR, independent of the supplemented precursor. Purity levels and protein yields after Ni-affinity chromatography were also the same (Figure S9). Specific activity of *Mm*CAR expressed with D- pantothenate increased from 0.25 to 0.85 U mg $^{-1}$, a 3.4-fold improvement. To confirm this result, *E. coli* K-12 MG1655 RARE (DE3) expressing *Mm*CAR in the presence of *Mm*PPTase were supplemented with 5 mM D- pantothenate and expressed at either 25°C or 28°C. Specific activities determined for purified enzyme preparations also resulted in increased specific activities (0.76 and 0.70 U mg $^{-1}$, Figure S10). The minor decrease in specific activity compared to CARs expressed at 20°C hints towards a new bottleneck.

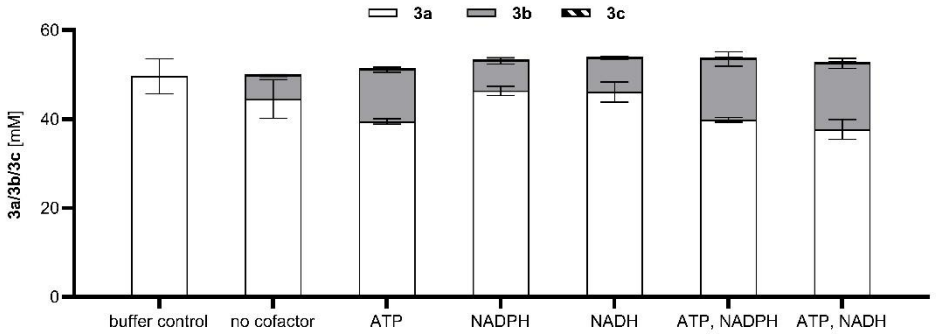

Figure 9. Bioreductions with or without addition of 10 mM cofactor. Biphasic bioconversions were conducted with 5 OD units of *E. coli* K-12 MG1655 RARE expressing *Mm*CAR and *Mm*PPTases and 50 mM **3a**, incubated at 28°C for 5 h on a tissue culture rotator. White: **3a**. Grey: **3b**. Black-striped: **3c** (see Figure 3 for reaction scheme). Error bars are shown for biological triplicates.

ATP and NADPH supply in whole cell biotransformations

Cofactor regeneration is essential for CAR reactions, rendering *in vivo* applications the most economic option. As discussed above, the decrease of CAR activity with time could be the result of various factors: deactivation of the CAR, depletion of cofactors, product inhibition, disintegration of membranes, cell lysis etc. Empiric cofactor feed experience showed that feed or extracellular recycling of NADPH had a positive effect on yields.[8] In order to investigate whether CAR deactivation or cofactor depletion was the major factor for stagnating conversion (Figure S2), external cofactors were added to bioreductions. Either 10 mM of ATP and/or NAD(P)H were added at the beginning of the bioreductions. This experiment should investigate whether the cells' metabolism for generating cofactors was sufficient to fuel the CAR reaction up to its full potential. In Figure 9, a trend of increased product yield by cofactor addition could be observed. Feed of both ATP and NAD(P)H increased product yield the most. Addition of ATP alone increased production more than feed of NAD(P)H alone (Figure 9). 14.9 mM of **3b** were produced by 5 OD units of *E. coli* K-12 MG1655 RARE (DE3) by adding 10 mM of ATP and NADPH and less than 1% of **3c** was detected. Supplementation of the reaction mix with ATP alone increased the product yield by 2.3-fold, whereas NAD(P)H addition did only slightly improve conversion as compared to the reaction without additional cofactors. Also extra NADH, the less costly alternative to NADPH, promotes CAR activity in whole cell bioreductions.[8] Based on these results, it can be concluded that the CAR reaction was limited in cofactor and could not unfold its full potential.

Addition of ATP and NADPH positively influenced **3b** yield, indicating that decreased metabolic activity was diminishing the reaction rate with time rather than CAR deactivation. To support whole cell-based cofactor recycling, an *in vitro* recycling system was coupled to standard biphasic bioconversions with 5 OD units of cells (Figure 10). The *in vitro* multi-enzyme system used was described to fully recycle ATP and NADPH and prevent undesired by-products (pyrophosphate, PP) in cell-free synthesis of aldehydes from acids.[31] Regeneration of ATP was achieved through the simultaneous action of polyphosphate kinases (PPK) from *Meiothermus ruber* and *Sinorhizobium meliloti* and NADPH was regenerated by a commercial glucose dehydrogenase (GDH- 105).[31] Enzymes used for the *in vitro* recycling of ATP and NADPH are listed in Table S4. All enzymes were expressed in *E. coli* MG1655 RARE (DE3) to keep background activities at a minimum. *Ec*PPase was added as cell free extract (CFE) to the reaction mix. *Mr*PPK and *Sm*PPK were enriched by Ni-affinity chromatography (Figure S11). The first attempt of combining the *in vitro* recycling system with the biphasic bioreduction showed promising results (Figure S12). Cell-mediated bioreductions showed high product formation even with substrate concentrations above 30 mM by utilizing only 5 OD units of cells.

***In vitro* recycling meets *in vivo* bioconversion**

The contribution of cellular metabolism for ATP/NADPH recycling was investigated by comparison of whole cells with the respective CFE. Therefore, bioreductions with 5 OD units or CFE samples equivalent to 5 OD units were incubated with the *in vitro* recycling system and compared. Notably, CFE samples of CAR incubated showed lower product yields (~65-72%, (Figure S12)) compared to the cell-based bioreductions. This could be due to higher initial reaction rates within the viable cell before the recycling system becomes effective or adds to the *in vivo* recycling of ATP and NADPH. To optimize ratios of regeneration enzymes for cell-based application, 2 equivalents of regeneration enzymes were compared to the standard set-up.[31] Product formation for 60 mM of **3a**, using the standard set-up, converted 24.4 mM of **3a**. Bioconversions with additional PPKs reached up to 40.9 mM conversion using twice the amount of PPKs for the regeneration of ATP (Nr.9 and 15 in Figure S12). 3.2% of **3c** was detected, which was most likely due to the high concentrations of recycling enzymes used and consequently more introduction of more background activity. In order to increase product formation, higher amounts of PPKs as previously described seemed beneficial.

The potential of cell-driven co-factor recycling combined with external ATP/NADPH recycling, was explored by monitoring reactions with various substrate concentrations of **3a** (10- 200 mM) (Figure 11). A direct comparison of bioreduction with and without recycling shows the impact of the recycling system.

After 41 h, bioreductions with 5 OD units without *in vitro* regeneration system produced 32.4 mM of **3b** and **3c** (4.2 g L^{-1})**,** including only 1.2% of **3c**. Hence, even after long incubation times, aldehyde overreduction was not predominant. Additionally, low biomass input was beneficial for mass balance. Testing higher substrate concentrations without the *in vitro* recycling system (data not shown) fully inhibited the reaction and showed only traces of **3b** and **3c** (4.05 mM of at 50 mM **3a** load). By contrast, full conversion was reached in the presence of the ATP/NADPH recycling system. Figure 11 shows that 89.2 mM of 100 mM **3a** were reduced with only 5 OD units of cells by applying *in vitro*

ATP/NADPH recycling in addition to cell mediated co-factor supply. Less than 1% of **3c** (0.78 mM) was detected even after 41 h of reduction. 89.2 mM product formation correspond to 11.42 g L^{-1} of **3b** and **3c** or a STY of 0.28 g L^{-1} h^{-1}. Up to the 24 h time point of incubation, the reaction proceeded at a constant reaction rate. The STY of the first 24 h was 0.418 g L^{-1} h^{-1}, emphasizing a high potential to produce fatty aldehydes. Even though the reaction rate decreased after 24 h of incubation, optimizations of the *in vitro* system prolonged cofactor supply and increased the reaction rate compared to the bioreductions without extracellular ATP/NADPH regeneration. Consequently, it pushed the reaction further and increased product formation in the presence of high substrate concentrations. This is the first time that significant product amounts were formed at 200 mM substrate concentration with only 5 OD units of cells.

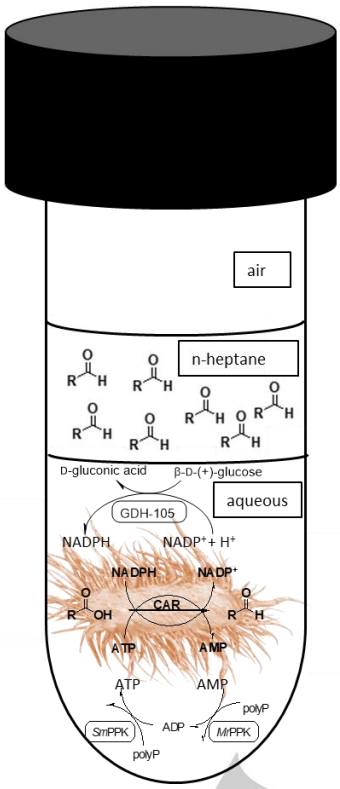

Figure 10. Biphasic bioreduction set-up with in vitro ATP/NADPH regeneration system. Adapted from Strohmeier et *al.*[31]

Summarizing, a major limiting factor in whole cell biotransformation is cellular metabolism. The impact of the stability of the carboxylate reductase requires further systematic investigations.

Preparative Gram scale production of aldehyde

Fluctuations of small-scale reactions in, e.g. pH, may impact the results. Feedback control for essential parameters can increase productivities significantly.[65] Our next aim was to upscale the reaction based on the extensive optimization of CAR mediated reduction of fatty acids. Hence, preparative biphasic bioreductions with cofactor regeneration under controlled conditions were performed in a bioreactor (450 mL reaction volume) with a total of 9.37 g of **3a** as the substrate (Figure S13A). After 27 h of incubation, 92.1% of the substrate was converted. The product comprised of only 1.6% of **3c** and 98.4% **3b**. A STY of 0.458 g L^{-1} h^{-1} was achieved. Temperature, pH, and agitation control (Figure S13B) as well as a reduction of the volume of the organic layer resulted in a faster conversion of **3a** (Figure S13A) as compared to the 1 mL scale reactions. The crude product in 650 mL of *n*-heptane, including 7.67 g of **3b**, was washed with $NaHCO_3$ and distilled. 10.4 g partially purified product was obtained. Lab-scale distillation resulted in a loss of 42% of **3b**. NMR and GC analysis (Figure S14) revealed that the product contained predominantly *n*-heptane, as well as very minor amounts of octanoic acid, 1-octanol and cell membrane-based long-chain fatty acids and/or derivatives. GC-FID analysis using calibration curves for quantification revealed that 4.67 g thereof was **3b.**

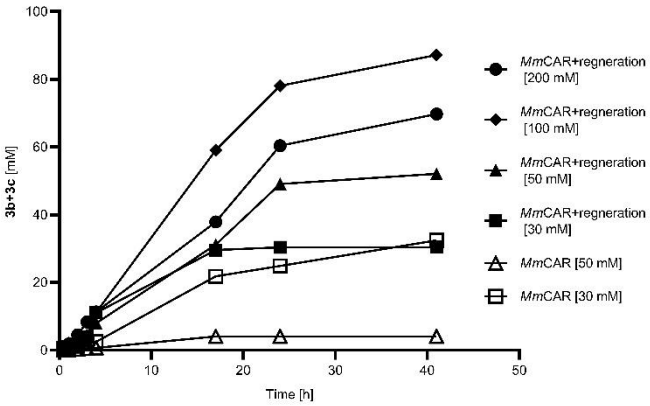

Figure 11. Biphasic bioreductions of **3a** with 5 OD units of *E. coli* K-12 MG1655 RARE expressing *Mm*CAR and *Mm*PPTase with external regeneration of ATP and NADPH. Bioconversions were incubated at 28°C for up to 41 h on a tissue culture rotator. Filled circle: 200 mM **3a** with regeneration system. Filled diamond: 100 mM **3a,** with regeneration system. Filled triangles: 50 mM **3a** with regeneration. Filled rectangles: 30 mM **3a** with regeneration system; Triangles: 50 mM **3a**, no regeneration system; Rectangles: 30 mM **3a**, no regeneration system. See Figure 3 for reaction scheme.

Improved cell viability by biocompatible organic layer

Due to ISPR, higher aldehyde concentrations were achieved and less alcohol as by-product was formed. However, not every solvent is suitable for a biphasic conversion. *n*-Heptane, the standard solvent used in this study, was reported to show hazardous attributes towards bacterial life, causing membrane perforation and leakage.[66] To avoid leakage and maintain the ability of cofactor regeneration, biocompatible solvents could be a solution. Therefore, a variety of non-water miscible biocompatible solvents were evaluated as second phase for ISPR. Product formation and cell viability were determined.

After biphasic bioreductions (Figure 12*),* selection pressure was applied on the used *E. coli* cells to screen for viable cells. Dilutions of 10^6 of cell suspension were plated, grown overnight at 37°C and colony forming units (CFUs) were counted (Figure 13). Only 25% of cells resuspended in reaction buffer containing 30 mM of **3a** and incubated for 5 h without a second phase (-solvent) survived compared to non- incubated cells without a carboxylic acid substrate.

n-Hexadecane showed no loss of CFUs for substrate **3a** compared to cells which were incubated in the tissue culture rotator for 5 h without any substrate and only a 25% of loss compared to cells with no substrate nor incubation. Also, farnesene showed promising results. In Brennan *et al.* also farnesene and dioctyl phthalate as well as *n*-hexadecane showed beneficial results regarding cell viability when *S. cerevisiae*

cultures were incubated with toxic substances.[67] Because *n*- hexadecane and farnesene delivered highest product titers of **3b** and **3c** (Figure 12) and showed improved viability after bioreductions with **3a** (Figure 13), these would be the most promising ISPR solvents. Recently, Yunus and Jones applied isopropyl myristate as a second layer for fatty alcohol production by reducing **3a** with *Mm*CAR and endogenous AHRs in *Synechocystis sp.* PCC 6803 strain as host organism.[19] According to our results and experiments reported,[67] the application of hexadecane would most likely also increase product titers in algae by maintaining viability and ability for essential cofactor regeneration for the CAR reaction.

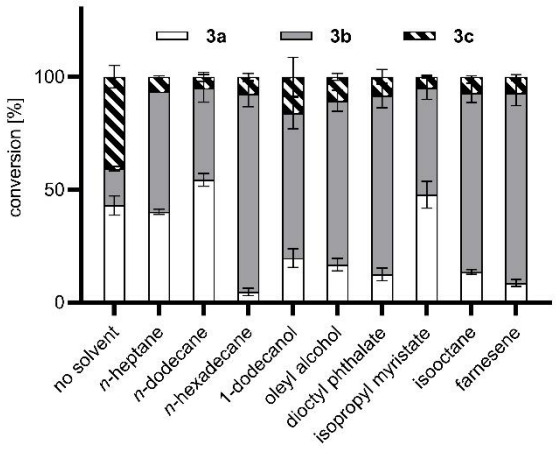

Figure 12. Biphasic bioreductions of 30 mM **3a** with 5 OD units of *E. coli* K-12 MG1655 RARE expressing *Mm*CAR and *Mm*PPTase using biocompatible solvents. Bioconversions were incubated at 28°C for 5 h on a tissue culture rotator. White: **3a**. Grey: **3b**. Black striped: **3c** (see Figure 3 for reaction scheme). Error bars are shown for biological triplicates.

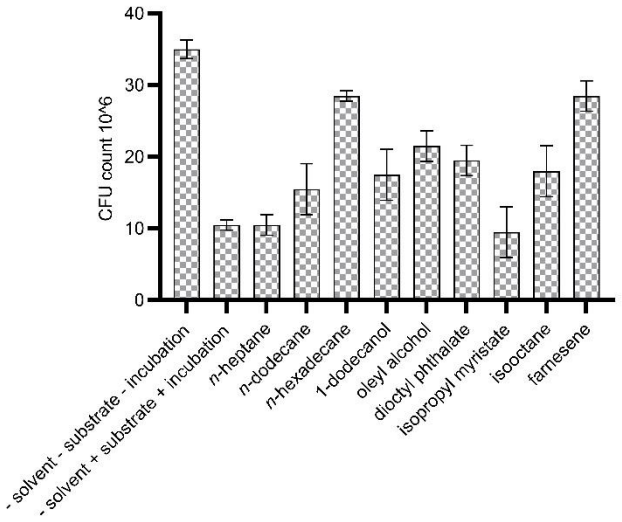

Figure 13. CFU count of plated 10^6 colonies of *E. coli* K-12 MG1655 RARE expressing *Mm*CAR and *Mm*PPTase after biphasic bioreduction of 30 mM **3a** with biocompatible solvents. Plates were incubated at 37°C for 5 h. Error bars are shown for triplicates.

Conclusion

Hardly any studies with the use of carboxylate reductases (CARs) *in vivo* were aiming for high aldehyde titres, and these were focused on aromatic aldehydes such as vanillin or piperonal.[18,34] Within this study, the main focus lay on the production of fatty aldehydes by CAR enzymes. We screened 15 fatty acid substrates with 5 CARs to find the most suited CAR for the desired application. *Mm*CAR showed the most promising and broadest substrate scope. Hence, *E. coli* expressing *Mm*CAR was used as the biocatalyst for a systematic optimization of various cultivation and reaction parameters, using octanoic acid (**3a**) as the substrate. Various bottlenecks were identified and strategies to circumvent these bottlenecks were evaluated in order to gain industrially relevant aldehyde yields. Schwendenwein *et al.* had shown that within 3 h, 30 mM piperonylic acid (**16a**) can be reduced by 50 g L^{-1} *E. coli* cells expressing *Nc*CAR and *Ec*PPTase, which corresponds to 1.5 g L^{-1} h^{-1}. Here we achieved similar productivities with 10 times less biocatalyst input and a non-tailored microbial host. In Table 4, relevant parameters are summarized. 92.1 mM of octanal (**3b)** and 1.54 mM of 1-octanol (**3c**) were produced within 27 h under controlled conditions. Overreduction was kept at only 1.6% without additional gene deletions. After isolation of the target compound from the organic layer, 4.67 g of octanal (**3b**) were obtained in a mixture with residual solvent. All together, this systematic investigation of the whole cell approach for medium- to long-chain fatty aldehyde production led to an approximate 16.6 times increase in productivity (from 0.745 g L^{-1} to 12.36 g L^{-1}), while using 10 times less biocatalyst.

The gradual improvement of whole cell bioreduction of octanoic acid (**3a**) is summarized in Table 4. By aiming for fatty aldehydes as the main product, toxicity effects in *E. coli* were addressed and circumvented by ISPR. We identified limitations in enzyme expression and post-translational modification, and improved CAR activation: Increased supply of 4´-phosphopantetheine, via increased CoA levels and a more suited PPTase improved activation of apo-CAR. The optimal PPTase for modifying the PCP- domain of *Mm*CAR originated also from *Mycobacterium marinum.*

During CAR expression in *E. coli*, limitations in CoA levels and possibly ATP levels constrained holo-CAR concentrations. During bioreduction, cofactor supply was also insufficient. Especially ATP supplementation improved whole cell conversion. Hence, a coupling of the whole cell biocatalyst with an *in vitro* regeneration system for ATP and NADPH produced more than 7 g L^{-1} of octanal (**3b**). To enhance productivity without applying an *in vitro* cofactor regeneration strategy, biocompatible solvents, e.g. *n*-hexadecane or farnesene, increased productivity by an increase in cell viability of *E. coli.* Most-likely they enable longer and more proficient cofactor regeneration and decreased membrane perforation. Due to overwhelming endogenous activity of alcohol dehydrogenases and aldo-keto reductases reducing the target aldehyde further to alcohol, a decreased biomass amount and a second organic layer were key to limit 1-octanol (**3c**) formation to below 1%.

Table 4. Summary of fatty aldehyde production[a] by whole cell biocatalyst.

parameter	single phase[b]	*n*-heptane[c]	reduced biomass[d]	*Mm*PPTase[e]	D-pantothenate[f]	ATP/NADPH supplementation[g]	5 OD +recycling[h]	controlled reaction (bioreactor)
substrate [mM]	6.0	50.0	10.0	10.0	30.0	50.0	100.0	100.0
Aldehyde and alcohol [mM]	5.82[f]	23.60	0.48	5.63	14.43	14.89	89.10	96.40
alcohol [% in product]	97.0	22.9	1.0	6.9	1.3	0.8	1.2	1.6
time [h]	4.5	18.00	5.00	3.00	16.00	5.00	41.00	27.00
productivity [g L^{-1}]	0.745	3.03	0.06	0.72	1.85	1.91	11.42	12.36
STY [g L^{-1} h^{-1}]	0.165	0.168	0.012	0.241	0.116	0.382	0.279	0.458
CWW [g]	0.050	0.050	0.005	0.050	0.005	0.005	0.005	1.000
biocatalyst yield [g g^{-1} CWW]	14.90	60.52	12.31	14.44	370.01	381.81	2284.70	12.36

[a] Bioreductions were carried out at 28°C on a tissue culture rotator.
[b] *Mm*CAR and *Ec*PPTase, 50 OD units.
[c] *Mm*CAR and *Ec*PPTase, 50 OD units, aqueous/*n*-heptane 1:1.
[d] *Mm*CAR and *Mm*PPTase, 5 OD units, aqueous/*n*-heptane1:1.
[e] *Mm*CAR and *Mm*PPTase expressed in the presence of 5 mM D-pantothenate, 5 OD units, aqueous/*n*-heptane 1:1.
[f] *Mm*CAR and *Mm*PPTase expressed in the presence of 5 mM D-pantothenate, 5 OD units, aqueous/*n*-heptane 1:1, addition of 10 mM ATP and/or NADPH.
[g] *Mm*CAR and *Mm*PPTase expressed in the presence of 5 mM D-pantothenate, 5 OD units, aqueous/*n*-heptane 1:1, addition of $NADP^+$, ATP, polyP, PPKs, GDH and PPase.
[h] *Mm*CAR and *Mm*PPTase expressed in the presence of 5 mM D-pantothenate, 5 OD units, aqueous/*n*-heptane 2:1, addition of $NADP^+$, ATP, polyP, PPKs, GDH and PPase in bioreactor.
[f] **3c** was used for calculating parameters. Less than 0.1% of **3b** was found due to overreduction.

Experimental Section

General: HPLC-MS grade acetonitrile was purchased from VWR. All other chemicals were obtained from Sigma–Aldrich or Roth and used without further purification. Exceptions are described below. Gasses for GC-analysis were obtained from Linde Gas, Austria

Strains, primers and enzymes: See Table S3-S5.

Cultivation and expression of *E. coli* strains harboring CAR enzymes (auto-induction protocol): Cultivation and expression procedures were performed as described previously.[68] The auto-induction medium LB 5052 with the appropriate antibiotic was inoculated with either 0.2% or 2% (v/v) inoculation volume and incubated at 37°C and 130 rpm for 4 h and the expression phase was conducted at 20°C, 25°C or 28°C for 12-14 h or 24 h.

For increasing the intracellular CoA pool, 5 mM of either L- valine, β- alanine, L- aspartic acid or D- pantothenic acid hemicalcium salt dissolved in ddH_2O was added before induction.

Cultivation and expression of *in vitro* cofactor recycling enzymes: *E. coli* K-12 MG1655 RARE cells were transfected with the plasmids listed in Table S4. Cultivation and expression was performed as described in Strohmeier *et al.*[31]

Expression analysis of CAR enzymes, cell disruption and Ni-affinity chromatography purification of enzymes: Methods were conducted as described in Horvat *et al.*[68]

Heat purification of *Gk*PPTase: Cell free extract (CFE) was prepared by resuspending the cell pellet of *E. coli* K-12 MG1655 RARE pMS470:*Gk*PPTase in 200 mM MES, pH 7.5. Cells were disrupted by ultrasonication and CFE prepared by centrifugation for 35 min at 65,563 rcf and 4°C. 1.5 mL of the CFE was incubated at 75°C for 10 min to purify *Gk*PPTase from non-thermostable *E. coli* background proteins. The CFE was then centrifuged for 30 min at 16,100 rcf and 4°C. The supernatant was used for *in vitro* 4´phosphopante-theinylation of apo-CAR to give active holo-CAR.

Additional activation of *Mm*CAR with *Gk*PPTase: Pre-activation: Partially purified *Mm*CAR (90 µg) was incubated with 1 mM CoA and 100 µg heat purified *Gk*PPTase at 28°C for 1 h and 500 rpm in an Eppendorf Thermomixer. For the assay, 6 mM 16a in KOH were added to 100 mM HEPES, pH 7.5, containing 10 mM $MgCl_2$. 30 µg of preactivated *Mm*CAR was added and the reduction started with 10 mM ATP and NADPH. This *in vitro* activity assay with preactivated CAR was incubated at 28°C for 3 h. The reaction was stopped by addition of 120 µL of MeOH and proteins removed by centrifugation at 16,100 rcf for 40 min. The supernatant was transferred into a microtiter plate and analyzed by HPLC-UV. As control, pre-activation reactions with *Gk*PPTase were incubated without CoA. Also, a buffer control was incubated at 28°C for 1 h.

Substrate scope of CARs - *in vitro:* Aliphatic acid substrate, 5 mM dissolved in DMSO, were added to 50 mM MES, pH 7.5, containing 10 mM $MgCl_2$. 90 µg of partially purified enzyme preparation (1 mg mL^{-1} of IMAC purified CARs) were added to the reaction mix. The reaction was started by addition of 1.2 mM ATP and NADPH. The *in vitro* activity assay was performed in a total volume of 600 µL in Eppendorf reaction tubes at 28°C and 700 rpm for 16-18 h in a Thermomixer. To stop the reaction, the solution was acidified to pH 2.0 with 3 M HCl. Extraction of fatty acid **a**, aldehyde **b** and alcohol **c** were achieved by two repeated extractions with equal amount of ethyl acetate, including 0.01% of *n*- tetradecane as internal standard (IS). Afterwards, the mixture was vortexed for 10 min and centrifuged for 15 min at 16,100 rcf and 4°C. The organic phase containing the extracted fatty **a**, **b**, **c**, and IS was transferred to a fresh Eppendorf tube and dried with Na_2SO_4 (approximately 10% (w/v)). 190 µL of the mixture were transferred into glass vials for GC analysis. The biotransformation reactions were carried out in technical

triplicates. Quantitation was performed based on linear interpolation of calibration curves with concentrations of standards from 0.156 mM to 10 mM.

Specific activity of CAR via NADPH-depletion monitoring: The NADPH depletion assay was used to determine initial rate activities for the reduction of aliphatic carboxylates as described,[68] however, carboxylic acids were dissolved in DMSO.

***In vivo* bioreduction of octanoic acid (3a):** Reactions with an immiscible solvent phase (*n*-heptane) were carried out in 15-mL Pyrex tubes and incubated at 28°C in a tissue culture tube rotator. The reactions with a total volume of 2 mL contained 500 mM HEPES or MES buffer, pH 7.5, supplemented with 100 mM glucose, 10 mM $MgSO_4$ and octanoic acid (**3a**), ranging from 1- 200 mM.

***In vivo* bioreduction of 3a with external co-factor supply:** The standard reaction contained **3a (**50 mM), 1 mM ATP, 0.5 mM $NADP^+$, 5 OD units of cells resuspended in 100 mM HEPES, pH 7.5, GDH-105 (0.2 U mL^{-1}), 100 mM β-D-glucose, 70 mM $MgCl_2$, 140 mM polyP (related to ortho-phosphate units, medium chain length: 25) (Merck), *Mr*PPK (100 µg mL^{-1}), *Ec*PPase (25 µg mL^{-1}) and *Sm*PPK (40 µg mL^{-1}). *Sm*PPK and *Mr*PPK were prepared and purified as described.[31] *Ec*PPase was used as cell-free lysate. Also, AMP (1 mM) was tested as catalytic cofactor. Additionally, the necessity of all components was tested by omitting one enzyme at the time.

Controlled bioreduction of 3a with *in vitro* co-factor regeneration in bioreactor: *E. coli* K-12 MG1655 RARE expressing *Mm*PPTase and *Mm*CAR were cultivated in TB-media and the autoinduction protocol using 2% inoculation volume and addition of 5 mM D-pantothenic acid hemicalcium salt prior induction.

1 g CWW (~1000 OD) was harvested and resuspended in 300 mM HEPES, pH 7.5. The reaction mix in a 1 L Biostat B unit (Sartorius) contained 3.13 g of **3a**, 1 mM ATP, 0.5 mM $NADP^+$, GDH-105 (0.2 U mL^{-1}), 100 mM β-D-glucose, 70 mM $MgCl_2$, 140 mM polyP (related to ortho-phosphate units, medium chain length: 25) (Merck), purified *Mr*PPK (300 µg mL^{-1}), CFE of *Ec*PPase (25 µg mL^{-1}) and purified *Sm*PPK (120 µg mL^{-1}) in an overall aqueous volume of 300 mL. Air was supplied with 0.3 L min^{-1} for the first 5 h to support cellular metabolism. 2M NaOH was used for pH regulation to pH 7.5. 150 mL of *n*-heptane was used as organic ISPR layer. Reactions were stirred at 300 rpm. Samples were analyzed at intervals. Bioreductions under controlled conditions were performed three times.

Purification of aliphatic compounds of controlled bioreduction and NMR analysis: After 27 h, the layers were separated by centrifugation at 15,039 rcf for 35 min. The aqueous layer was extracted once with 100 mL of *n*-heptane. The combined *n*-heptane fractions, containing **3a**, **3b** and **3c**, were washed three times with saturated $NaHCO_3$ solution to remove unreacted octanoic acid. *n*-Heptane was removed in a fractional distillation apparatus, equipped with a water-cooled condenser. The overhead vapor temperature did not exceed 98°C. 10.4 g of partially purified product was obtained and analyzed via gas chromatography-flame ionization detection (GC-FID) and NMR. The product was composed of 44% octanal (**3b**) in residual *n*-heptane, as quantified by GC-FID. For recording NMR spectra a Bruker Avance III 300 MHz FT NMR spectrometer with autosampler was used (^{1}H: 300.36 MHz; ^{13}C: 75.5 MHz). The residual protonated solvent signals serve as internal standard for interpretation of the chemical shifts δ. To facilitate the interpretation, the C-spectra were proton decoupled. In addition, 2D spectra (H,H-COSY, HSQC and HMBC) were recorded for identification and confirmation of the structure. Deuterated solvents were purchased from euriso-top®.

^{1}H NMR (300 MHz, $CDCl_3$) δ 9.75 (s, 1H, CHO), 2.50 – 2.32 (m, 2H, $CO-CH_2$-), 1.70 – 1.51 (m, 2H, $CO-CH_2-CH_2$-), 1.40 – 1.13 (m, J = 7.5 Hz, 21H, -CH_2- octanal and heptane), 0.87 (t, J = 6.5 Hz, 11H, -CH_3, octanal and heptane) ppm.

^{13}C NMR (75.5 MHz, $CDCl_3$) δ 203.0 (CHO), 44.1 ($CO-CH_2$-), 32.0 (2 CH_2, heptane), 31.8 (CH_2), 29.3 (CH_2), 29.2 (2 CH_2, **3b** and heptane), 22.8 (2 CH_2, heptane), 22.7 (CH_2), 22.3 (CH_2), 14.2 (2 CH_3, heptane), 14.2 (CH_3) ppm.

GC-FID analysis (method 1): GC-FID measurements were performed for substances for which product standards were available (Table S6). A ZP-5 column (crosslinked 5% Ph-Me Siloxane; 30 m, 0.32 mm in diameter and 0.25 µm film thickness) on a Shimadzu GC 2010 Plus equipped with an FID was used. Sample aliquots of 1 µL were injected in split mode (split ratio 10:1) at 240°C injector temperature and 320°C detector temperature with N_2 as carrier gas. The temperature program for quantification of **3a**/**3b**/**3c** was as follows: hold at 70°C for 4 min, followed by temperature gradients to 130°C at 5°C min^{-1} and to 300°C at 45°C per min^{-1} and a hold at 300°C for 2 min. The total runtime for **3a**/**3b**/**3c** was 21.45 min. This method was adapted for C6, C7, C9, C10 C11, C11:1 and C16:1 fatty acids/aldehydes/alcohols. The total run time ranged from 14.75 to 21.45 min. GC-FID results were evaluated with the GC-FID Data Analysis software LabSolution by Shimadzu.

GC-FID analysis for biocompatible solvents: Biocompatible solvents are characterized by relatively high boiling points and their retention times interfered especially with long-chain substrate and/or product peaks or internal standard. Individual method adjustments were made to the main method (method 2). A list of solvents and corresponding methods used is given in Table S9.

GC-MS analysis: Gas chromatography-mass spectrometry (GC-MS) measurements were performed for substances for which only the substrate was available. A detailed list of retention times and structures is summarized in Table S7. An Optima 1 MS (100% dimethylpolysiloxane; 30 m, 0.25 mm in diameter and 0.25 µm film thickness) on a Shimadzu GCMS-QP2010 SE equipped with a mass selective detector was used. Sample aliquots of 1 µL were injected in split mode (split ratio 6.5:1) at 240°C injector temperature and 320°C detector temperature with helium as carrier gas. The oven temperature program was as follows: 70°C for 5 min and a temperature gradient to 300°C at 15°C min^{-1} followed by a hold for 5 min at 300°C. The total run time was 24.26 min. The mass selective detector was operated in a mass range of 30-500 m/z and an ionization voltage of 70 eV. GC-MS results were evaluated with the GC-MS Shimadzu Data Analysis software LabSolution.

HPLC-UV detection of 16a, b and c: Measurements were performed by HPLC-UV. Equipment and method used are described in Horvat *et al*.[68] Retention times and chemical structure are shown in Table S8.

Acknowledgements

The authors thank Anna Katharia Migglautsch for the workup of the prep-scale reaction, Daniel Schwendenwein for identifing limitations in the correlation of expression and activities of CARs, Fredi Brühlmann and Andreas Taglieber

for valuable discussions and Kristala L.J. Prather for providing *E. coli* K-12 MG1655 RARE (DE3). The Austrian Research Agency FFG (P860262) and Firmenich SA are kindly acknowledged for financial support.

Keywords: fatty acids • carboxylic acid reductase • green chemistry • aldehydes • enzymatic reduction *in vivo*

[1] E. Vosnaki, "Perfume Shrine: Myth Debunking 1: What Are Aldehydes, How do Aldehydes Smell and Chanel No.5," **2008**.
[2] D. Meyer, L. Walter, G. Kolter, M. Pohl, M. Müller, K. Tittmann, *J. Am. Chem. Soc.* **2011**, *133*, 3609–3616.
[3] Z. Zhu, Y. J. Zhou, M. K. Kang, A. Krivoruchko, N. A. Buijs, J. Nielsen, *Metab. Eng.* **2017**, *44*, 81–88.
[4] Y. Hu, Z. Zhu, J. Nielsen, V. Siewers, S. V. Hu Yating , Zhu Zhiwei, Nielsen Jens, *Open Biol.* **2019**, *9*, 190049.
[5] J. R. Hanson, *J. Organomet. Chem.* **1992**, *426*, 22–23.
[6] N. Butler, A. M. Kunjapur, *J. Biotechnol.* **2020**, *307*, 1–14.
[7] A. He, T. Li, L. Daniels, I. Fotheringham, J. P. N. Rosazza, *Appl. Environ. Microbiol.* **2004**, *70*, 1874–1881.
[8] K. Napora-Wijata, K. Robins, A. Osorio-Lozada, M. Winkler, *ChemCatChem* **2014**, *6*, 1089–1095.
[9] J. M. Choi, S. S. Han, H. S. Kim, *Biotechnol. Adv.* **2015**, *33*, 1443–1454.
[10] M. Winkler, *Curr. Opin. Chem. Biol.* **2018**, *43*, 23–29.
[11] M. Moura, D. Pertusi, S. Lenzini, N. Bhan, L. J. Broadbelt, K. E. J. Tyo, *Biotechnol. Bioeng.* **2016**, *113*, 944–952.
[12] W. Finnigan, A. Thomas, H. Cromar, B. Gough, R. Snajdrova, J. P. Adams, J. A. Littlechild, N. J. Harmer, *ChemCatChem* **2017**, *9*, 1005–1017.
[13] D. Gahloth, M. S. Dunstan, D. Quaglia, E. Klumbys, M. P. Lockhart-cairns, A. M. Hill, S. R. Derrington, N. S. Scrutton, N. J. Turner, D. Leys, *Nat. Chem. Biol.* **2017**, *13*, 975–981.
[14] P. Venkitasubramanian, L. Daniels, J. P. N. Rosazza, *J. Biol. Chem.* **2007**, *282*, 478–485.
[15] J. Beld, E. C. Sonnenschein, C. R. Vickery, J. P. Noel, M. D. Burkart, *Nat. Prod. Rep.* **2014**, *31*, 61–108.
[16] L. E. N. Quadri, P. H. Weinreb, M. Lei, M. M. Nakano, P. Zuber, C. T. Walsh, *Biochemistry* **1998**, *37*, 1585–1595.
[17] J. Hansen, E. H. Hansen, H. P. Sompalli, J. Sheridan, J. Heal, W. Hamilton, *Composition and methods for the biosynthesis of vanillin beta-D-glucoside*, **2013,** WO2013022881 A1.
[18] E. H. Hansen, B. L. Møller, G. R. Kock, C. M. Bünner, C. Kristensen, O. R. Jensen, F. T. Okkels, C. E. Olsen, M. S. Motawia, J. Hansen, *Appl. Environ. Microbiol.* **2009**, *75*, 2765–74.
[19] I. S. Yunus, P. R. Jones, *Metab. Eng.* **2018**, *49*, 59–68.
[20] Y. J. Zhou, N. A. Buijs, Z. Zhu, J. Qin, V. Siewers, J. Nielsen, *Nat. Commun.* **2016**, *7*, 11709.
[21] A. Abghari, S. Chen, *Front. Energy Res.* **2014**, *2*, 21.
[22] P. Sattayawat, I. Sofian Yunus, P. R. Jones, I. S. Yunus, P. R. Jones, *Proc. Natl. Acad. Sci.* **2020**, *117*, 1404–1413.
[23] J. Rosenblatt, R. A. Reitzel, N. Vargas-Cruz, A. M. Chaftari, R. Hachem, I. Raad, *Front. Microbiol.* **2017**, *8*, 1999.
[24] B. K. Yoon, J. A. Jackman, E. R. Valle-González, N. J. Cho, *Int. J. Mol. Sci.* **2018**, *19*, 1114.
[25] L. A. Royce, P. Liu, M. J. Stebbins, B. C. Hanson, L. R. Jarboe, *Appl. Microbiol. Biotechnol.* **2013**, *97*, 8317–8327.
[26] P. Liu, A. Chernyshov, T. Najdi, Y. Fu, J. Dickerson, S. Sandmeyer, L. Jarboe, *Appl. Microbiol. Biotechnol.* **2013**, *97*, 3239–3251.
[27] M. K. Akhtar, N. J. Turner, P. R. Jones, *PNAS* **2013**, *110*, 87–92.
[28] M. Ahsan, S. Sung, H. Jeon, M. Patil, T. Chung, H. Yun, *Catalysts* **2017**, *8*, 4.
[29] S. Maurer, H. Schewe, J. Schrader, M. Buchhaupt, *J. Biotechnol.* **2019**, *305*, 11–17.
[30] A. M. Kunjapur, Y. Tarasova, K. L. J. Prather, *J. Am. Chem. Soc.* **2014**, *136*, 11644–11654.
[31] G. A. Strohmeier, I. C. Eiteljörg, A. Schwarz, M. Winkler, *Chem. - A Eur. J.* **2019**, *25*, 6119–6123.
[32] W. Finnigan, R. Cutlan, R. Snajdrova, J. P. Adams, J. A. Littlechild, N. J. Harmer, *ChemCatChem* **2019**, *11*, 3474–3489.
[33] J. Citoler, S. R. Derrington, J. L. Galman, H. Bevinakatti, N. J. Turner, *Green Chem.* **2019**, *21*, 4932–4935.
[34] D. Schwendenwein, G. Fiume, H. Weber, F. Rudroff, M. Winkler, *Adv. Synth. Catal.* **2016**, *358*, 3414–3421.
[35] J. M. Woodley, M. Bisschops, A. J. J. Straathof, M. Ottens, *J. Chem. Technol. Biotechnol.* **2008**, *83*, 121–123.
[36] B. Bühler, I. Bollhalder, B. Hauer, B. Witholt, A. Schmid, *Biotechnol. Bioeng.* **2003**, *81*, 683–694.
[37] M. Horvat, G. Fiume, S. Fritsche, M. Winkler, *J. Biotechnol.* **2019**.
[38] T. Li, J. P. N. Rosazza, *J. Bacteriol.* **1997**, *179*, 3482–3487.
[39] M. Winkler, C. K. Winkler, *Monatshefte für Chemie - Chem. Mon.* **2016**, *147*, 575–578.
[40] H. Stolterfoht, D. Schwendenwein, C. W. Sensen, F. Rudroff, M. Winkler, *J. Biotechnol.* **2017**, *257*, 222–232.
[41] D. Gahloth, G. A. Aleku, D. Leys, *J. Biotechnol.* **2020**, *307*, 107–113.
[42] A. N. Khusnutdinova, R. Flick, A. Popovic, G. Brown, A. Tchigvintsev, B. Nocek, K. Correia, J. C. Joo, R. Mahadevan, A. F. Yakunin, *Biotechnol. J.* **2017**, *12*, 1–12.
[43] S. Sarria, N. S. Kruyer, P. Peralta-Yahya, *Nat. Biotechnol.* **2017**, *35*, 1158–1166.
[44] M. J. Sheppard, A. M. Kunjapur, K. L. J. Prather, *Metab. Eng.* **2016**, *33*, 28–40.
[45] N. Tsukagoshi, R. Aono, *J. Bacteriol.* **2000**, *182*, 4803–4810.
[46] M. A. Fraatz, M. Goldmann, T. Geissler, E. Gross, M. Backes, J.-M. Hilmer, J. Ley, J. Rost, A. Francke, H. Zorn, *J. Agric. Food Chem.* **2016**, acs.jafc.6b04793.
[47] Y. Xu, F. Li, K. Yang, Y. Qiao, Y. Yan, J. Yan, *Energy Convers. Manag.* **2019**, *181*, 501–506.
[48] P. Kallio, A. Pásztor, K. Thiel, M. Kalim Akhtar, P. R. Jones, M. K. Akhtar, P. R. Jones, *Nat. Commun.* **2014**, *5*, 1–8.
[49] T. Baba, T. Ara, M. Hasegawa, Y. Takai, Y. Okumura, M. Baba, K. A. Datsenko, M. Tomita, B. L. Wanner, H. Mori, *Mol. Syst. Biol.* **2006**, *2*, 2006.0008.
[50] N. A. Sophos, V. Vasiliou, *Chem. Biol. Interact.* **2003**, *143–144*, 5–22.
[51] I. Moreno-Gonzalez, C. Soto, *Semin. Cell Dev. Biol.* **2011**, *22*, 482–487.
[52] M. A. Post-Beittenmiller, K. M. Schmid, J. B. Ohlrogge, *Plant Cell* **1989**, *1*, 889–899.
[53] K. Magnuson, S. Jackowski, C. O. Rock, J. E. Cronan, *Microbiol. Rev.* **1993**, *57*, 522–542.
[54] H. Stolterfoht, G. Steinkellner, D. Schwendenwein, T. Pavkov-Keller, K. Gruber, M. Winkler, *Front. Microbiol.* **2018**, *9*, 250.
[55] Z. Hu, *Methods and Compositions for Producing Fatty Alcohols*, **2010**, US20100105963 A1.
[56] A. Thomas, R. Cutlan, W. Finnigan, M. van der Giezen, N. Harmer, *Nat. Commun. Biol.* **2019**, *2*, 429.
[57] A. M. Kunjapur, B. Cervantes, K. L. J. J. Prather,

Biochem. Eng. J. **2016**, *109*, 19–27.
[58] R. Leonardi, S. Jackowski, *EcoSal Plus* **2007**, *2*, 3.6.3.4.
[59] G. Dallner, *Chem. Phys. Lipids* **2011**, *164*, S12.
[60] M. Yun, C. G. Park, J. Y. Kim, C. O. Rock, S. Jackowski, H. W. Park, *J. Biol. Chem.* **2000**, *275*, 28093–28099.
[61] D. S. Vallari, S. Jackowski, C. O. Rock, *J. Biol. Chem.* **1987**, *262*, 2468–2471.
[62] T. P. Begley, C. Kinsland, E. Strauss, *Vitam. Horm.* **2001**, *61*, 157–171.
[63] J. M. Williamson, *Methods Enzymol.* **1985**, *113*, 589–595.
[64] R. V. Vadali, G. N. Bennett, K. Y. San, *Metab. Eng.* **2004**, *6*, 133–139.
[65] R. Simutis, A. Lübbert, *Biotechnol. J.* **2015**, *10*, 1115–1130.
[66] J. Sikkema, J. A. M. De Bont, B. Poolman, *Microbiol. Rev.* **1995**, *59*, 201–222.
[67] T. C. R. Brennan, C. D. Turner, J. O. Krömer, L. K. Nielsen, *Biotechnol. Bioeng.* **2012**, *109*, 2513–2522.
[68] M. Horvat, S. Fritsche, R. Kourist, M. Winkler, *ChemCatChem* **2019**, *11*, 4171–4181.

10.1002/cctc.202000895

Entry for the Table of Contents

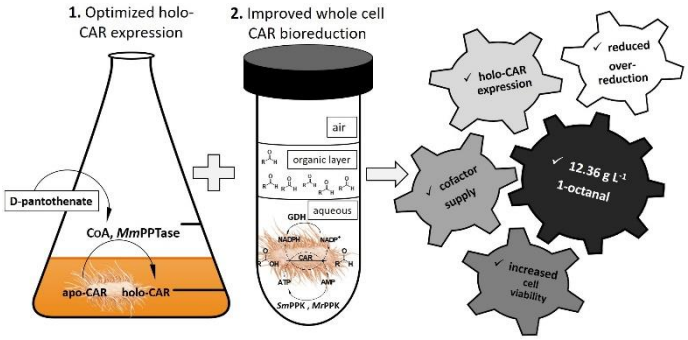

A mild, sustainable and selective biocatalytical approach to aldehydes is presented. Carboxylic acid reductases (CARs) were employed for fatty acid (C6-C18) reduction. Cell viability, cofactor supply, functional expression, and in-situ product removal were systematically investigated and 12.36 g L^{-1} of octanal was produced from octanoic acid